International Journal of Numerical Methods for Heat & Fluid Flow

Mixing of electrokinetically-driven power-law fluids in zigzag microchannels

Ching-Chang Cho Cha'o-Kuang Chen Her-Terng Yau

Mixing of electrokinetically-driven power-law fluids in zigzag microchannels

Ching-Chang Cho
Department of Vehicle Engineering, National Formosa University, Yunlin, Taiwan
Cha'o-Kuang Chen
Department of Mechanical Engineering, National Cheng Kung University, Tainan, Taiwan, and
Her-Terng Yau
Department of Electrical Engineering, National Chin-Yi University of Technology, Taichung, Taiwan

Received 2 April 2013
Revised 11 May 2013
Accepted 6 June 2013

Abstract

Purpose – The purpose of this paper is to study the mixing performance of the electrokinetically-driven power-law fluids in a zigzag microchannel.

Design/methodology/approach – The Poisson-Boltzmann equation, the Laplace equation, the modified Cauchy momentum equation, and the convection-diffusion equation are solved to describe the flow characteristics and mixing performance of power-law fluids in the zigzag microchannel. A body-fitted grid system and a generalized coordinate transformation method are used to model the grid system and transform the governing equations, respectively. The transformed governing equations are solved numerically using the finite-volume method.

Findings – The mixing efficiency of dilatant fluids is higher than that of pseudoplastic fluids. In addition, the mixing efficiency can be improved by increasing the width of the zigzag blocks or extending the total length of the zigzag block region.

Originality/value – The results presented in this study provide a useful insight into potential strategies for enhancing the mixing performance of the power-law fluids in a zigzag microchannel. The results of this study also provide a useful source of reference for the development of efficient and accurate microfluidic systems.

Keywords Electroosmotic flow, Microchannel, Mixing, Non-newtonian fluid, Power-law fluid

Paper type Research paper

1. Introduction

In recent years, microfluidic systems have found widespread use for such applications as chemical and biological analyses, drug delivery, DNA hybridization and so on. Generally, the samples in microfluidic systems are transported by an electric field (i.e. electroosmotic flow, EOF), a pressure force, a surface tension, and so on. Of these methods, EOF is commonly preferred due to the plug-like velocity profile, the lack of moving parts and the high repeatability and reliability. Thus, it is essential that the flow characteristics and transport performance of EOF are thoroughly understood in order to optimize the microfluidic devices.

The authors would like to thank the National Science Council of the Republic of China, Taiwan, for financially supporting this research under Contract Nos. 101-2221-E-006-092-MY2 and NSC 101-2811-E-006-057.

0961-5539
DOI 10.1108/HFF-04-2013-0107

In the literature, most EOF investigations consider Newtonian fluids (Patankar and Hu, 1998; Arnold *et al.*, 2008; Nithiarasu and Lewis, 2008; Yau *et al.*, 2011; Cho *et al.*, 2012a). However, in many practical microfluidic applications, the rheological behavior of the fluids must be considered since the used fluids have the non-Newtonian characteristics (e.g. bio-fluids). Therefore, the study of non-Newtonian EOF has attracted increasing attention in recent years. Zhao *et al.* (2008) analyzed the EOF of power-law fluids in a slit microchannel. They have derived a generalized model for the Smoluchowski velocity. Their results showed that the Smoluchowski velocity monotonically decreases with an increasing flow behavior index. Tang *et al.* (2009) performed a numerical investigation into the EOF of power-law fluids in a straight microchannel. The results showed that the rheological behavior of the fluid has a significant effect on the flow field pattern. Hadigol *et al.* (2011) examined the mixed electroosmotic/pressure-driven flow of a power-law fluid in a slit microchannel with a non-uniform zeta potential distribution. It was shown that the fluid behavior index in the power-law model has a significant effect on the flow characteristics. Babaie *et al.* (2011) performed a numerical investigation into the EOF flow of power-law fluids through a slit microchannel in the presence of a pressure gradient. The results showed that for pressure-assisted flow, shear-thinning fluids reach a higher velocity than shear-thickening fluids, whereas the reverse is true when an adverse pressure gradient is applied. Cho *et al.* (2012b) performed a numerical investigation into the EOF of power-law fluids in a rough microchannel characterized by a complex-wavy surface. The results showed that the flow behavior of non-Newtonian fluids is significantly dependent on the value of the flow behavior index in the power-law model. It also showed that the flow behavior is affected by the surface roughness.

Generally, the performance of many microfluidic systems is fundamentally dependent on the mixing efficiency of the samples. However, obtaining a rapid and efficient mixing effect in microfluidic devices is difficult since the small characteristic scale of the microchannels constrains the fluid flow to the low Reynolds number regime. To enhance the mixing performance in the microfluidic devices, many researchers have focussed on the investigation of micromixing scheme. These proposed schemes for enhancing mixing performance can be broadly classified as either active or passive. In active mixing schemes, the samples are mixed via the application of external time-varying perturbation forces, e.g., pressure perturbations (Niu and Lee, 2003), electrical perturbations (Cho *et al.*, 2012c), magnetic stirring perturbations (Ryu *et al.*, 2004), and so forth. In passive mixing schemes, the samples are mixed by specifically-designed geometries, e.g., staggered herringbone microchannels (Stroock *et al.*, 2002), three-dimensional serpentine microchannels (Liu *et al.*, 2000), waveform microchannels (Chen and Cho, 2007) and so on. Overall, the studies presented in (Niu and Lee, 2003; Cho *et al.*, 2012c; Ryu *et al.*, 2004; Stroock *et al.*, 2002; Liu *et al.*, 2000; Chen and Cho, 2007) considered a Newtonian fluid and showed that the proposed schemes can effectively enhance the mixing efficiency in microfluidic devices.

As described above, most fluids in microfluidic systems have non-Newtonian characteristics. However, most existing investigations into the micromixing schemes only consider Newtonian fluids. In other words, the literature lacks a detailed investigation into the mixing characteristics of non-Newtonian fluids in microchannels. Accordingly, the present study investigates the micromixing characteristics of non-Newtonian fluids in a zigzag microchannel. In performing the study, the rheological behavior of the non-Newtonian fluid is characterized using a power-law model. The study focusses specifically on the respective effects on the mixing performance of the flow behavior index in the power-law model and geometry parameters of the microchannel.

2. Mathematical formulation

2.1 Governing equations and boundary conditions

When polar solutions come into contact with microchannel surfaces, an electrical double layer (EDL) is formed adjacent to the channel wall. If an external electric field is applied to the microchannel, an electrokinetic driving force is induced, which causes the solution within the channel to flow. When analyzing the flow behavior within the microchannel, the electrokinetic driving force must be taken into account. Therefore, the flow behavior and mixing performance in the microchannel can be governed by the Poisson-Boltzmann equation, the Laplace equation, the modified Cauchy momentum equation, and the convection-diffusion equation. To simplify the governing equations, the following assumptions are made: the samples are incompressible fluids and have the same diffusion coefficient; the gravitational and buoyancy effects are sufficiently small to be ignored; no chemical reactions take place; the Joule heating effect is ignored; and the flow field is two-dimensional and in a steady state. Given these assumptions, the governing equations can be written as follows (Cho *et al.*, 2012b):

$$\nabla^2\psi = \frac{2n_0 ze}{\varepsilon\varepsilon_0}\sinh\left(\frac{ze}{k_B T_a}\psi\right), \tag{1}$$

$$\nabla^2\phi = 0, \tag{2}$$

$$\nabla\cdot\vec{V} = 0, \tag{3}$$

$$\rho\left(\vec{V}\cdot\nabla\right)\vec{V} = -\nabla p + \nabla\cdot\mu\left[\nabla\vec{V} + \left(\nabla\vec{V}\right)^T\right] + 2n_0 ze\sinh\left(\frac{ze}{k_B T_a}\psi\right)\nabla(\psi+\phi), \tag{4}$$

$$\left(\vec{V}\cdot\nabla C\right) = D\nabla^2 C, \tag{5}$$

where ψ is the potential induced by the charge on the walls, n_0 is the bulk concentration of the ions, z is the ionic valence, e is the elementary charge, ε is the dielectric constant of the electrolyte solution, ε_0 is the permittivity of a vacuum, k_B is the Boltzmann constant, T_a is the absolute temperature, ϕ is the applied electric potential, ρ is the fluid density, $\vec{V}$ is the velocity vector, p is the pressure, C is the sample concentration, D is the diffusion coefficient and superscript T denotes transposition. Note that the last term in Equation (4) represents the electrokinetic driving body force. In addition, μ presented in Equation (4) is the dynamic viscosity. In this study, the dynamic viscosity is expressed using the power-law model, i.e., (Cho *et al.*, 2012):

$$\mu = m\dot{\gamma}^{n-1}, \tag{6}$$

where m is the flow consistency index, n is the flow behavior index, and $\dot{\gamma}$ is the shear rate. According to Equation (6), the fluid can present different flow behavior depending on the flow behavior index. Generally, the fluid is said to be pseudoplastic if $n < 1$, Newtonian if $n = 1$ or dilatant if $n > 1$.

As shown in Figure 1, it is assumed that the two samples are injected electrokinetically into the microchannel via two separate inlets. A constant electric potential is applied at the two inlets and a reference electric potential is set at the outlet.

Meanwhile, a constant zeta potential and a no-slip velocity boundary condition are imposed on all the wall surfaces. The boundary conditions at the inlets, outlet and wall surface are therefore specified as follows.

Inlets:

$$\nabla\psi\cdot\vec{n}_{\perp}=0,\ \phi=\phi_{in};\ p=0;\ C=C_A \text{ or } C_B;$$

Outlet:

$$\nabla\psi\cdot\vec{n}_{\perp}=0,\ \phi=\phi_{out};\ p=0;\ \nabla C\cdot\vec{n}_{\perp}=0;$$

Wall surface:

$$\psi=\zeta,\ \nabla\phi\cdot\vec{n}_{\perp}=0,\ \vec{V}=0;\ \nabla C\cdot\vec{n}_{\perp}=0;$$

where ϕ_{in} and ϕ_{out} are the externally applied electric potentials at the inlets and outlet, respectively; C_A and C_B are the concentrations of samples A and B, respectively; ζ is the zeta potential on the wall surface; and $\vec{n}_{\perp}$ denotes the normal vector.

2.2 Numerical method

The geometry configuration shown in Figure 1 is a non-orthogonal system. Therefore, in analyzing the flow in the microchannel, the governing equations given in Equations (1)-(5) must be transformed from a Cartesian coordinate system to a generalized curvilinear coordinate system. The transformed governing equations have the following generalized form (Cho *et al.*, 2012a, b):

$$\frac{\partial}{\partial\xi}(\rho_t U_t f)+\frac{\partial}{\partial\eta}(\rho_t V_t f)=\frac{\partial}{\partial\xi}\left[\frac{\Gamma_t}{J}\left(\alpha_t\frac{\partial f}{\partial\xi}-\beta_t\frac{\partial f}{\partial\eta}\right)\right]+\frac{\partial}{\partial\eta}\left[\frac{\Gamma_t}{J}\left(-\beta_t\frac{\partial f}{\partial\xi}+\gamma_t\frac{\partial f}{\partial\eta}\right)\right]+JS_t, \quad (7)$$

where f is a generalized variable; ξ and η are the two axes of the transformed coordinate system; $U_t=\left(\frac{\partial y}{\partial\eta}u-\frac{\partial x}{\partial\eta}v\right)$ and $V_t=\left(\frac{\partial x}{\partial\xi}v-\frac{\partial y}{\partial\xi}u\right)$ are the velocity components in the transformed coordinate system; S_t is a source term; $\alpha_t=\left[\left(\frac{\partial x}{\partial\eta}\right)^2+\left(\frac{\partial y}{\partial\eta}\right)^2\right]$, $\beta_t=\left[\left(\frac{\partial x}{\partial\xi}\right)\left(\frac{\partial x}{\partial\eta}\right)+\left(\frac{\partial y}{\partial\xi}\right)\left(\frac{\partial y}{\partial\eta}\right)\right]$ and $\gamma_t=\left[\left(\frac{\partial x}{\partial\xi}\right)^2+\left(\frac{\partial y}{\partial\xi}\right)^2\right]$ are parameters of the transformed coordinates, respectively; and $J=\left[\left(\frac{\partial x}{\partial\xi}\right)\left(\frac{\partial y}{\partial\eta}\right)-\left(\frac{\partial x}{\partial\eta}\right)\left(\frac{\partial y}{\partial\xi}\right)\right]$ is the Jacobian factor. Note that prior to solving the transferred governing equations, a grid system is need to be generated. In the study, the grid system is generated by solving the set of Poisson equations (Thomas and Middlecoff, 1980), i.e.:

$$\frac{\partial^2\xi}{\partial x^2}+\frac{\partial^2\xi}{\partial y^2}=P_c(\xi,\eta) \quad (8a)$$

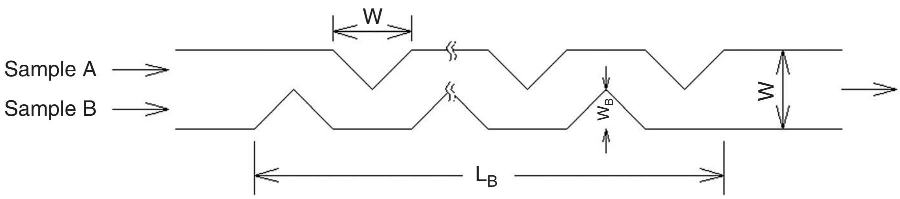

Notes: W, width of the microchannel; W_B, width of the zigzag blocks; L_B, total length of the zigzag block region

Figure 1.
Schematic illustration of zigzag microchannel

$$\frac{\partial^2\eta}{\partial x^2}+\frac{\partial^2\eta}{\partial y^2}=Q_c(\xi,\eta) \tag{8b}$$

where $P_c(\xi,\eta)$ and $Q_c(\xi,\eta)$ are the control parameters of mesh distribution. In this study, the two parameters are determined according to (Thomas and Middlecoff, 1980).

In performing the simulations, the governing equations and boundary conditions were solved using the finite-volume numerical method (Patankar, 1980). A second-order scheme was used to discretize the convection terms and the velocity and pressure fields were coupled using the SIMPLE (semi-implicit method for pressure-linked equations) algorithm (Patankar, 1980). Finally, the discretized algebraic equations were solved iteratively using a line-by-line TDMA (tri-diagonal matrix algorithm) scheme until a convergent solution was achieved.

3. Results and discussion

In performing the simulations, it was assumed that the zeta potential had a magnitude of $\zeta=-30mV$ and was uniformly distributed along the wall surface. In addition, the electric field strength was set as $E=100$ V/cm, the flow consistency index was given as $m=1\times10^{-3}Pa\cdot s^n$, and the diffusion coefficient of the two samples was set as $D=1\times10^{-10}m^2s^{-1}$. The other physical properties of the fluid were specified as follows: fluid density, $\rho=10^3kgm^{-3}$; Boltzmann constant, $k_B=1.38\times10^{-23}JK^{-1}$; absolute temperature, $T_a=300K$; permittivity of vacuum, $\varepsilon_0=8.854\times10^{-12}Fm^{-1}$; dielectric constant of medium, $\varepsilon=80$; elementary charge, $e=1.6021\times10^{-19}C$; and ionic valency, $z=1$. Finally, the non-dimensional Debye-Huckel parameter (defined as $\kappa=\mathrm{K}\times W$, where $K^{-1}=\left(\frac{2n_0z^2e^2}{\varepsilon\varepsilon_0k_BT_a}\right)^{-1/2}$ is the characteristic thickness of the EDL) was assigned a value of $\kappa=100$.

To validate the numerical codes, the numerical results for the u-velocity profiles in a parallel-plate channel were compared with the corresponding analytical solutions. Given the assumption of Debye-Huckel linearization, the analytical solutions for the u-velocity distributions are given by (Zhao *et al.*, 2008; Cho *et al.*, 2012b):

$$u=-\frac{\varepsilon\varepsilon_0\zeta E}{m}\left[1-\frac{\cosh(Ky)}{\cosh(KL_c)}\right],\quad \text{for } n=1.0. \tag{9a}$$

$$u=\frac{K}{2}\left(-\frac{\varepsilon\varepsilon_0\zeta E}{m}\right)^2\times\frac{\sinh(2KL_c-\sinh(2Ky)-2(KL_c-Ky))}{2\cosh^2(KL_c)},\quad \text{for } n=0.5. \tag{9b}$$

Figure 2 compares the numerical and analytical results for the non-dimensional u-velocity distributions in the parallel-plate channel. It is seen that a good agreement exists between the two sets of results.

Figures 3(a) and (b) show the distributions of the flow streamlines and sample concentration, respectively, in the zigzag microchannel. As stated in Section 2, an electrokinetic driving force is generated by the interaction between EDL potential and the externally-applied electric field. Since the EDL is only formed near the wall surface, the electrokinetic driving force acts only on the fluid near the wall surface. Because no extra driving force is considered in the microchannel, the bulk fluid is dragged into motion via the electrokinetic driving force. As a result, the flow streamlines follow the profile of the wall surface and no flow separation is observed (see Figure 3(a)). In addition, since the small characteristic scale of the channel constrains the fluid flow

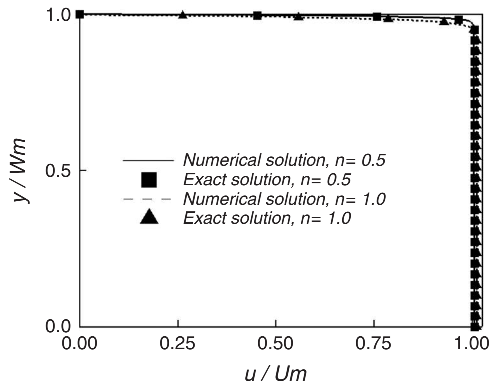

Notes: The non-dimensional Debye-Huckel parameter is specified as $k = 100$; *Um*, the mean velocity in the microchannel

Figure 2. Comparison of exact and numerical solutions for non-dimensional *u*-velocity distributions in parallel-plate microchannel

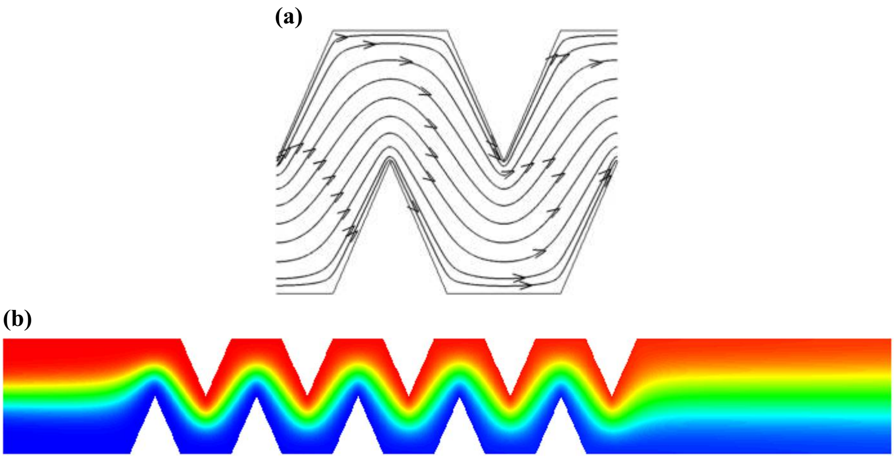

Notes: $W_B = 0.5W$, $L_B = 10W$ and $n = 0.7$

Figure 3. (a) Flow streamlines and (b) sample concentration distribution in zigzag microchannel

to the low Reynolds number regime, the samples mixing occur as a result of diffusion. As the samples flow through the zigzag microchannel, the interfacial contact area between samples is increased, and thus the diffusion effect is improved. Consequently, the mixing performance is enhanced (Figure 3(b)).

Figure 4 shows the variation of the mixing efficiency with the flow behavior index. Note that the mixing efficiency (η_m) is evaluated in accordance with (Cho *et al.*, 2012c; Chen and Cho, 2007):

$$\eta_m = \left[1 - \frac{\int_0^W |C - C_\infty| d\eta}{\int_0^W |C_0 - C_\infty| d\eta}\right] \times 100\%, \tag{10}$$

where C is the sample concentration, and C_0 and C_∞ are the sample concentrations in the completely unmixed and completely mixed conditions, respectively. As defined in

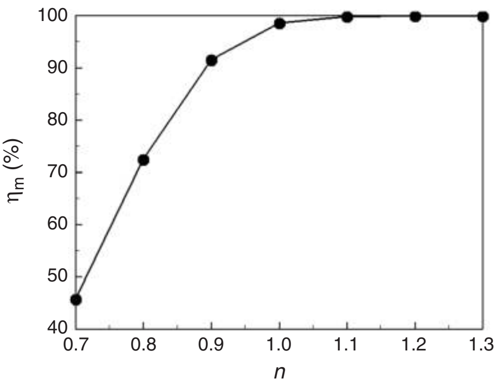

Notes: $W_B = 0.5W$ and $L_B = 10W$

Figure 4. Variation of mixing efficiency at $x = 30W$ with flow behavior index

Equation (6), the viscosity increases with an increasing flow behavior index. As a result, the flow velocity decreases as the flow behavior index is increased, and thus a longer mixing time occur. Consequently, the mixing efficiency increases with an increasing flow behavior index. In other words, the dilatant fluids (i.e. $n > 1.0$) has a higher mixing efficiency than the pseudoplastic fluids (i.e. $n < 1.0$).

Figure 5 shows the variation of the mixing efficiency with the width of the zigzag blocks as a function of flow behavior index. Note that in the figure, the mixing performance of pseudoplastic fluids is only discussed since the dilatant fluids and Newtonian fluid have had a high mixing efficiency (see Figure 4). As the width of the zigzag blocks increases, the interfacial contact area between the samples is increased. Therefore, a better diffusion effect can be obtained. As a result, it is shown that the mixing efficiency increases as the width of the zigzag blocks is increased.

Figure 6 shows the variation of the mixing efficiency with the length of the zigzag block as a function of flow behavior index. It is expected that extending the total length of zigzag block region increases the interfacial contact area between the samples, and thus the diffusion effect is enhanced. Consequently, the mixing efficiency improves as the total length of the zigzag block region is extended.

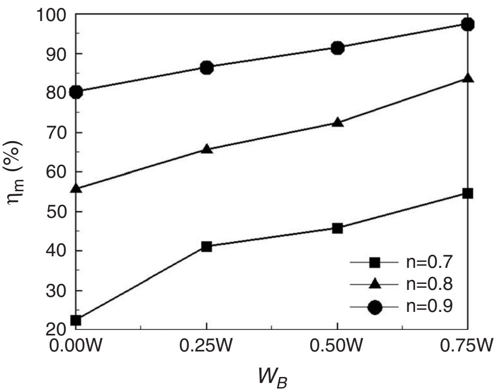

Note: $L_B = 10W$

Figure 5. Variation of mixing efficiency at $x = 30W$ with width of zigzag blocks as function of flow behavior index

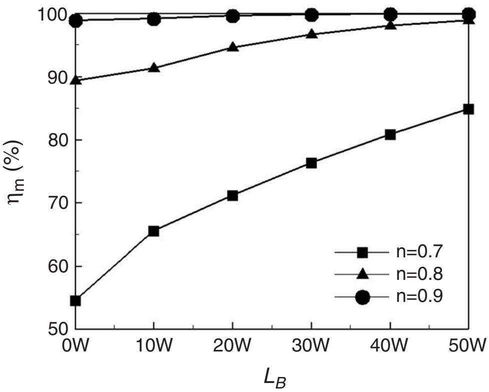

Figure 6.
Variation of mixing efficiency at $x = 70W$ with total length of zigzag block region as function of flow behavior index

Note: $W_B = 0.5W$

4. Conclusions

This paper has investigated the mixing characteristics of electrokinetically-driven non-Newtonian fluids through a zigzag microchannel. In the study, the power-law model was used to characterize the rheological behavior of the non-Newtonian fluid. The effects on the mixing performance of the geometry parameters and flow behavior index in the power-law model have been explored. The results have shown that the flow behavior index has significant effect on the mixing performance. The results have been shown that the mixing performance can be improved by increasing the width of the zigzag blocks or extending the total length of the zigzag block region.

References

Arnold, A.K., Nithiarasu, P. and Tucker, P.G. (2008), "Finite element modeling of electro-osmotic flows on unstructured meshed", *International Journal of Numerical Methods for Heat & Fluid flow*, Vol. 18 No. 1, pp. 67-82.

Babaie, A., Sadeghi, A. and Saidi, M.H. (2011), "Combined electroosmotically and pressure driven flow of power-law fluids in a slit microchannel", *Journal of Non-Newtonian Fluid Mechanics*, Vol. 166 Nos 14/15, pp. 792-798.

Chen, C.K. and Cho, C.C. (2007), "Electrokinetically-driven flow mixing in microchannels with wavy surface", *Journal of Colloid and Interface Science*, Vol. 312 No. 2, pp. 470-480.

Cho, C.C., Chen, C.L. and Chen, C.K. (2012a), "Characteristics of combined electroosmotic flow and pressure-driven flow in microchannels with complex-wavy surfaces", *International Journal of Thermal Sciences*, Vol. 61, pp. 94-105.

Cho, C.C., Chen, C.L. and Chen, C.K. (2012b), "Electrokinetically-driven non-newtonian fluid flow in rough microchannel with complex-wavy surface", *Journal of Non-Newtonian Fluid Mechanics*, Nos 173/174, pp. 13-20.

Cho, C.C., Chen, C.L. and Chen, C.K. (2012c), "Mixing enhancement in crisscross micromixer using aperiodic electrokinetic perturbing flows", *International Journal of Heat and Mass Transfer*, Vol. 55 Nos 11/12, pp. 2926-2933.

Hadigol, M., Nosrati, R. and Raisee, M. (2011), "Numerical analysis of mixed electroosmotic/pressure driven flow of power-law fluids in microchannels and micropumps", *Colloids and Surfaces A: Physicochemical and Engineering Aspects*, Vol. 374 Nos 1-3, pp. 142-153.

Liu, R.H., Stremler, M.A., Sharp, K.V., Olsen, M.G., Santiago, J.G., Adrian, R.J., Aref, H. and Beeber, D.J. (2000), "Passive mixing in a three-dimensional serpentine microchannel", *Journal of Microelectromechanical Systems*, Vol. 9 No. 2, pp. 190-197.

Nithiarasu, P. and Lewis, R.W. (2008), "A short note on Joule heating in electro-osmotic flows a consistent non-dimensional scaling", *International Journal of Numerical Methods for Heat & Fluid flow*, Vol. 18, Nos 7-8, pp. 919-931.

Niu, X. and Lee, Y.K. (2003), "Efficient spatial-temporal chaotic mixing in microchannels", *Journal of Micromechanics and Microengineering*, Vol. 13 No. 3, pp. 454-462.

Patankar, S.V. (1980), *Numerical Heat Transfer and Fluid Flow*, McGraw-Hill, New York, NY.

Patankar,N.A. and Hu, H.H. (1998), "Numerical simulation of electroosmotic flow", *Analytical Chemistry*, Vol. 70 No. 9, pp. 1870-1881.

Ryu, K.S., Shaikh, K., Goluch, E., Fan, Z. and Liu, C. (2004), "Micro magnetic stir-bar mixer integrated with parylene microfluidic channels", *Lab on a Chip*, Vol. 4 No. 6, pp. 608-613.

Stroock, A.D., Dertinger, S.K.W., Ajdari, A., Mezic, I., Stone, H.A. and Whitesides, G.M. (2002), "Chaotic mixer for microchannels", *Science*, Vol. 295 No. 5555, pp. 647-651.

Tang, G.H., Li, X.F., He, Y.L. and Tao, W.Q. (2009), "Electroosmotic flow of non-Newtonian fluid in microchannels", *Journal of Non-Newtonian Fluid Mechanics*, Vol. 157 Nos 1/2, 133-137.

Thomas, P.D. and Middlecoff, J.F. (1980), "Direct control of the grid point distribution in meshes generated by elliptic equations", *AIAA Journal*, Vol. 18 No. 6, pp. 652-656.

Yau, H.T., Wang, C.C., Cho, C.C. and Chen, C.K. (2011), "A numerical investigation into electroosmotic flow in microchannels with complex wavy surfaces", *Thermal Science*, Vol. 15, Supplement 1, pp. S87-S94.

Zhao, C., Zholkovskij, E., Masliyah, J.H. and Yang, C. (2008), "Analysis of electroosmotic flow of power-law fluids in a slit microchannel", *Journal of Colloid and Interface Science*, Vol. 326 No. 2, pp. 503-510.

Corresponding author
Professor Her-Terng Yau can be contacted at: pan1012@ms52.hinet.net